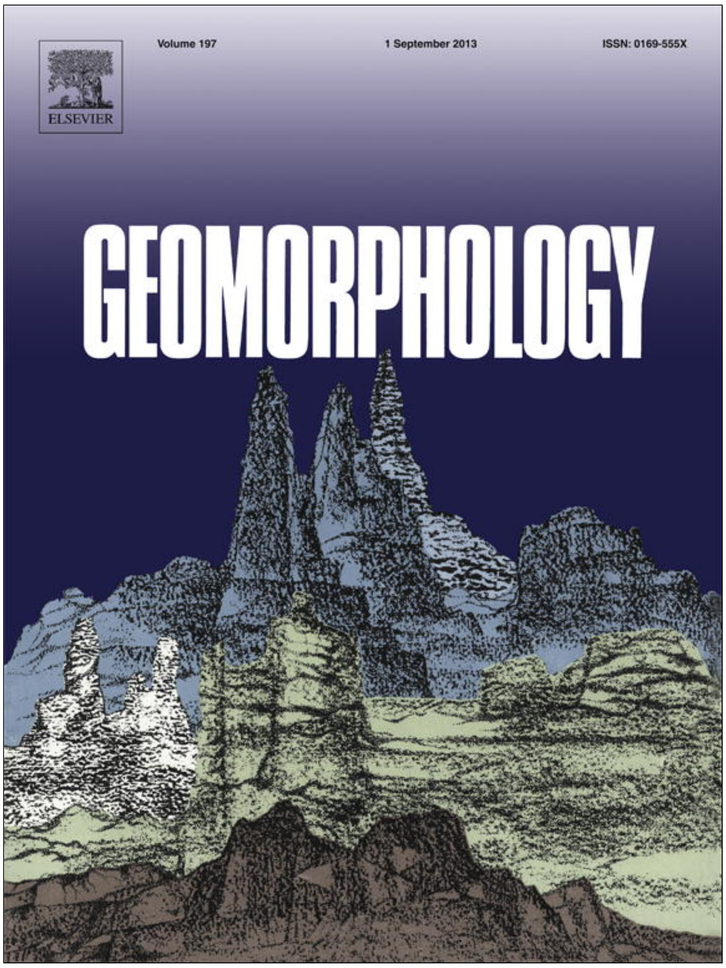
Volume 197
1 September 2013
ISSN: 0169-555X
ELSEVIER
GEOMORPHOLOGY

Geomorphology 197 (2013) 137–144

Contents lists available at SciVerse ScienceDirect

Geomorphology

journal homepage: www.elsevier.com/locate/geomorph

Effects of water erosion on the redistribution of soil organic carbon in the hilly red soil region of southern China

Xue Zhang [a,b], Zhongwu Li [a,b,*], Zhenghong Tang [c], Guangming Zeng [a,b], Jinquan Huang [a,b], Wang Guo [a,b], Xiaolin Chen [a,b], Aaron Hirsh [d]

[a] College of Environmental Science and Engineering, HunanUniversity, Changsha 410082, PR China
[b] Key Laboratory of Environmental Biology and Pollution Control, HunanUniversity, Ministry of Education, Changsha 410082, PR China
[c] Community and Regional Planning Program, 313 Architecture Hall, College of Architecture, University of Nebraska—Lincoln, Lincoln, NE 68588-0105, USA
[d] Civil Engineering Program, N104 Scott Engineering Center, College of Engineering, University of Nebraska—Lincoln, Lincoln, NE 68588-6105, USA

ARTICLE INFO

Article history:
Received 25 October 2011
Received in revised form 18 March 2013
Accepted 9 May 2013
Available online 17 May 2013

Keywords:
Soil erosion
Simulation rainfall
Soil organic carbon (SOC)
Redistribution
Infiltration
Red soil

ABSTRACT

Water erosion processes can significantly affect the delivery and distribution patterns of soil organic carbon (SOC) within the landscape. While many studies focus on the erosion processes and runoff transport of SOC, little attention has been paid to the on-site redistribution and vertical transport of SOC. This study characterizes SOC erosion dynamics, including infiltration-associated movement, and discusses the effects of rainfall intensity and slope position on SOC transport within the hilly red soil region of southern China. The results show that SOC loss was likely due to sediment transport rather than runoff. The eroded SOC was not significantly enriched, which may be due to the soil properties and the type of rainfall event. The initial SOC concentration affected the enrichment ratio of eroded SOC in the sediment. On-site horizontal redistribution occurred regardless of rainfall intensity, whereas the SOC transport trends varied with rainfall intensity and slope positions. This demonstrates that soil preservation could reduce SOC loss, and thus influence the global carbon cycle.

1. Introduction

Despite the significant effect soil erosion has upon the global carbon cycle (Stallard, 1998), the most widespread form of soil erosion and degradation is a highly debated and uncertain topic (Lal et al., 1998; Lal, 2003; Lal and Pimentel, 2008). In the past decade, researchers have investigated the impact of erosion upon soil carbon, soil loss, as well as the associated carbon dynamics during rainfall. For example, Polyakov and Lal (2004) found that soil organic carbon (SOC) concentration in runoff decreases within creasing rainfall duration. Pan and Shangguan (2006) reported that soils in grasslands have higher percolation and provide less runoff and sediment than those in croplands. Seybold et al. (2002) found that soils not subjected to tillage are characterized by higher infiltration rates. While these studies reflect a range of complicated erosion processes that affect soil, they also focus on the impacts that land management practices can have on surface runoff, soil loss, and percolation (Seybold et al., 2002; Pan and Shangguan, 2006; Rimal and Lal, 2009). The behavior of SOC in different soil layers with varying infiltration processes has not been directly detected, and therefore the SOC vertical transport process is not completely understood.

SOC loss during erosion is affected by many factors such as soil properties, rainfall intensity/duration, topography, surface cover, and soil wetness (Foster and Wischmeier, 1974). Many rainfall simulation experiments have focused on the effects of rainfall intensity on soil erosion. For instance, Jin et al. (2009) reported that higher rainfall intensities produce more sediment and, consequently, higher nutrient losses and lower sediment SOC enrichment ratios (ER_{SOC}). The research of Jacinthe et al. (2004) confirmed that soil erosion associated with intense rainstorms affects the loss of labile SOC. Topography can strongly influence both soil erosion and SOC distribution. Upperslope positions are generally eroded while lower positions are depositional (McCarty and Ritchie, 2002; Papiernik et al., 2005). Soil nutrients accumulate in depositional areas (Heckrath et al., 2005; Papiernik et al., 2007), and therefore, SOC concentrations are usually higher at the lower slope positions.

The main factors that affect water erosion and the resultant SOC loss processes have been intensively studied in the past (Engel et al., 2009; Jin et al., 2009; Rimal and Lal, 2009). In a previous study conducted in a tropical area (Rumpel et al., 2009), carbon exporting processes including horizontal redistribution, vertical transport, and sediment runoff were detected. However, the soil layer was too thin (10 mm) to confirm the vertical transport process, and the climate and soil conditions differed from those in a subtropical region. In this study, we attempt to (i) provide insight into the temporal patterns of sediment, runoff, and SOC discharge for rainfall events of varying intensities; (ii) determine the on-site redistribution of SOC

* Corresponding author at: College of Environmental Science and Engineering, Hunan University, Changsha 410082, PR China. Tel./fax: +86 731 88640078.
E-mail address: lizw@hnu.edu.cn (Z. Li).

0169-555X/$ – see front matter © 2013 Elsevier B.V. All rights reserved.
http://dx.doi.org/10.1016/j.geomorph.2013.05.004

along a slope; and (iii) verify the vertical transport of SOC within soil layers. From this, dynamic patterns of SOC concentrations and loading at the plot level can be determined.

2. Material and methods

2.1. Study site

Soil profiles for ten provinces in Southern China were examined in this study. These areas are characterized by red soil, which covers a total area of 2.18 × 10^6 km^2 (Zhao, 2002). Due to the subtropical conditions in the so-called "hilly red soil region," red soils are often heavily weathered and low in SOC (Shi et al., 2010). Water erosion occurs throughout this region, with raindrop splash and slope runoff erosion being the dominant mechanisms (Tang, 2004). Although the total amount of soil loss is lower than that of the Chinese Loess Plateau, the thin soil layer available for plant growth in the red soil hilly region can cause severe erosion conditions. The large geographic area of the hilly red soil region also makes it an important component of China's terrestrial carbon cycle.

This study was carried out at the soil and water conservation research station of Shaoyang (111°22′E, 27°03′N) in the southwest–central part of Hunan Province, China (Fig. 1). The research station is situated upstream of the Zi River, within the hinterland of the Hengshao Basin. The average yearly temperature and the mean annual precipitation of the station are 17.1 °C and 1327.5 mm, respectively. The region's soil is Quaternary red clay with a clay-to-loam texture (Yang et al., 1989), which is considered an Ultisol according to the U.S. Soil Taxonomy. The soils are generally low in organic matter concentrations, as is typical for the hilly red soil region.

2.2. Plot set-up and rainfall simulation

In 2009, a 5 m × 5 m land block was chosen as the experimental area (Fig. 2). The land block was previously planted with slope-cultivated *Polygonatum odoratum* (Mill.) Druce. After harvesting the crops, the land was disked several times to smooth the soil surface and then laid fallow. One year later, the slope of the land block was found to be slightly S-shaped, with a mean slope gradient of 15°. The mean SOC concentration of the 20 cm thick surface layer was

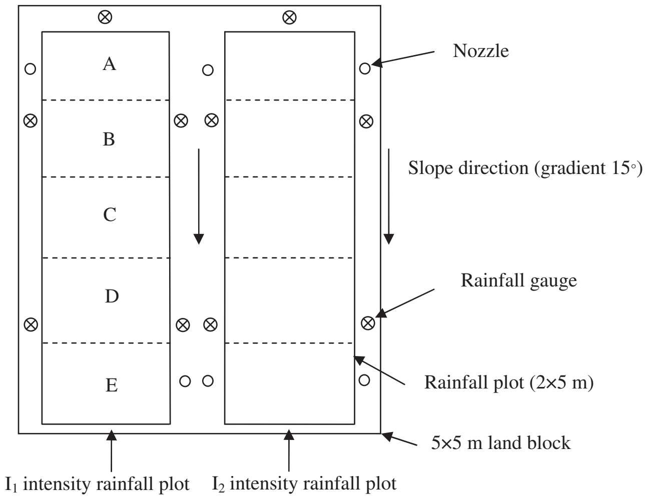

Fig. 2. Plot design for the rainfall simulation experiments.

4.39 ± 0.42 g kg^{-1} (the mean value of 15 replicate plots ± standard error). The total nitrogen and phosphorus concentrations of the soil were 0.60 ± 0.05 and 0.79 ± 0.12 g kg^{-1}, respectively. The soil had a clay-loamy texture with 16.72 ± 0.83% clay particle size distribution, 27.50 ± 0.45% silt, and 55.77 ± 0.63% sand. During the summer of 2010, two 2 m × 5 m plots were delimited for the rainfall simulation experiment (Fig. 2). Each plot was bound with a thin metal frame driven into the ground in order to prevent runoff from adjacent areas. The lower end of each plot was equipped with a funnel-shaped collection trough that channeled runoff into a marked 2.5 L pail. The plots were designed to have (i) minimal soil disturbance during the boundary setting; and (ii) minimal local soil variations, which was achieved through the minimization of the distance between the plots. The upper part of each plot was the sediment and carbon source while the bottom parts typically accumulated any carbon that had not yet reached the outlet.

For the erosion experiments, a rainfall simulator with a SPRACO cone jet nozzle mounted on the top of fixed 4.57 m long stand pipes was built. The nozzles were placed on the boundary of the plots

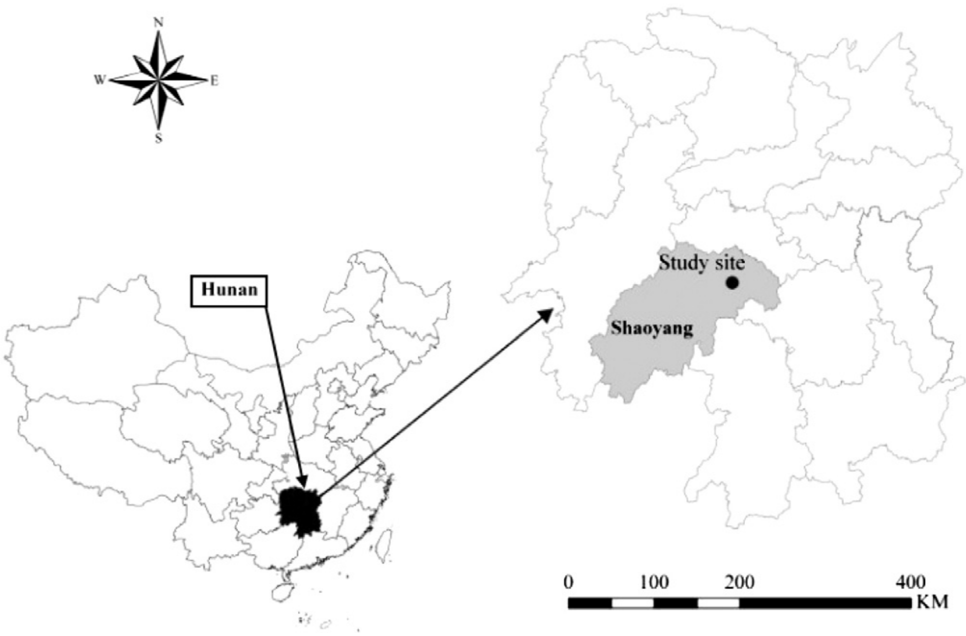

Fig. 1. Location of the study area.

(Fig. 2). The median drop size was 2.4 mm with a uniformity of 89.7%. For the experiments on the two plots, rainfall intensities of 0.5–0.7 and 1.5–1.7 mm min^{-1} were used, representing the low and high intensity storms of this region.

Starting at the beginning of the rainfall, the time at which runoff first occurred was measured using a chronometer. Once overland surface runoff began, random runoff samples were manually and intermittently collected at 3 min intervals using a 1000 mL kettle. The runoff samples were treated with a solution (HCl, 37.5%) to accelerate coagulation. All other runoff and sediment samples were collected in a marked pail, which was changed several times, and the total runoff volume in 3 min was recorded. Excess water was then decanted. The samples in the kettles were taken to the laboratory. After settling for 24 h in collectors, the runoff water was separated, and the sediment was collected. The sediment was dried in an oven at 105 °C for 24 h and then weighed. The dried sediment samples were ground for a SOC analysis, and the water was filtered for a TOC analysis. The duration of each rainstorm was 30 min after the initiation of runoff. The actual rainfall intensity and uniformity was determined using five rain gauges at borders of the plot (Fig. 2). After the simulated rainfall event, the actual rainfall intensity was determined. The mean rainfall intensity was found to be 0.58 mm min^{-1} for the I_1 event plot and 1.64 mm min^{-1} for the I_2 event plot.

2.3. Sampling

The two rainfall plots were divided into five subplots (A to E) at 1 m equal intervals (Fig. 2). To estimate the vertical SOC transport during rainstorms, soil was sampled in both plots at depths of 0–5, 5–10, 10–20, and 20–35 cm. Before the rainfall experiment, three separately arranged grids were chosen as the three replicates in each subplot. Each grid had a dimension of 20 cm × 20 cm, and samples at each grid and depth were taken using a 70 mm diameter corer. The boreholes were later filled and carefully leveled in order to reduce the effects of soil sampling. After the rainfall experiment, soils were also sampled in the same manner. With this strategy, three replicated soil samples were obtained (about 2 kg) that were representative of each subplot and each depth, from both plots, before and after the rainfall.

2.4. Sample treatment and analysis

All sediment and soil samples were dried, crushed to pass through a 2 mm sieve, and thoroughly mixed. Finally, the dry mass was transported to the Hunan Agricultural Government for chemical analysis. SOC concentrations were determined with the dichromate oxidation method of Walkley and Black (1934); total nitrogen concentrations were measured by the Kjeldahl (1883) method; and the total phosphorus concentrations were measured using the Kara et al. (1997) method. Soil particle sizes were analyzed using the pipette method (Gee and Bauder, 1986). TOC concentrations in the runoff samples were measured with an IL 550 TOC-TN analyzer.

2.5. Statistical analysis

Statistical data analysis was performed using SPSS 16.0 for Windows. ANOVA was used to detect the effects of slope position. Differences in soil properties among different slope positions were detected using the least significant difference procedure for a multiple range test at the 0.05 significance level.

3. Results

3.1. Surface runoff, sediment transport, and associated organic carbon

The time required for the initiation of runoff differed with rainfall intensity. When the intensity was 0.58 mm min^{-1} (I_1 event) runoff started at 4′34″, whereas under a 1.64 mm min^{-1} (I_2 event) event the runoff start time was only 1′31″ (Table 1). Through the trials, three stages of sediment transport and runoff loss were distinguished. In the first stage, all rain water was infiltrated, and no runoff and sediment loss occurred. In the second stage, runoff started, and the rates of sediment and runoff loss rapidly increased. In the third stage (approx. 14 min) both sediment loss and runoff loss rates reached steady values regardless of rainfall intensity. During this stage, the lowest peak value of sediment loss rate was observed (22′34″ for the I_1 event and 19′31″ for the I_2 event). Although the simulated rainfall was stopped 30 min after the initiation of runoff, the runoff continued for a period longer than 30 min thereafter. Following the last 3 min of sampling, more runoff samples were collected, although the sediment load became too low to weigh. Consequently, only runoff loss rates are available for this period. Sediment and runoff were seen to accumulate more rapidly during the I_2 event than the I_1 event, and the overall variation of sediment yield was similar to that of runoff for both rainfall intensities (Table 1).

SOC concentration in the sediment and runoff samples changed with respect to time during each of the rainfall simulations (Table 2). During the I_2 event SOC concentrations in the sediment were initially high, but diminished rapidly within a short period of time, and then fluctuated until the end of the experiment. Between 7′31″ and 10′31″ sediment SOC concentrations decreased as rapidly as 3.06 g kg^{-1} min^{-1}. During the first period of the I_1 event decreases in both sediment and runoff SOC concentrations were less marked, and the values fluctuated sharply during the rainfall event.

Changes in concentration with respect to time were found to be very different for the sediment SOC verses the runoff SOC (Table 2), in that, the former shows strong fluctuations, while the latter is relatively constant. The loss rate of sediment SOC for the I_1 event was very low, and consistently remained lower than 0.5 g min^{-1}. In the I_2 event, sediment SOC concentration initially increased until 7′52″, after which it then fluctuated toward lower levels. The quicker surface runoff start time resulted in faster losses of soil and carbon.

Fig. 3 shows the change in ER_{soc} during each rainfall simulation. ER_{soc} for the I_2 event was initially high but diminished within a short period, eventually reaching relatively low values with minor fluctuations. This trend was less obvious for the I_1 event. During the first 18 min of the I_2 event, ER_{soc} remained >1, and then stabilized to values <1. For the I_1 event, values of ER_{soc} were <1 throughout the experiment.

The quantity of sediments and SOC exported from the plots was found to be related to rainfall intensity. From the I_1 and I_2 events, 2.25 and 11.24 kg of sediments containing 3.18 and 56.09 g SOC were collected, respectively, at the outlet of the plots. In addition, 8.64×10^4 and 3.93×10^5 mL of runoff, containing 2.81 and 13.55 g of dissolved carbon respectively, were collected.

3.2. Horizontal redistribution of SOC

Redistribution of total SOC was calculated for the 0–20 cm deep soil layer (Fig. 4). Prior to the I_1 event, the SOC concentration was significantly different among slope positions ($P = 0.000$). The concentration in subplot A was considerably higher than those in subplots B and C, but lower than that in subplot E ($P = 0.001$–0.009). The SOC concentration was significantly higher in subplot E than in all other positions ($P < 0.05$). SOC redistribution occurred due to the I_1 event. The SOC concentration in subplot B was substantially lower than those in subplots D and E, while the SOC in subplot C was significantly lower than that of subplot E ($P = 0.039$–0.010). The SOC concentration in both upper (subplot A) and lower (subplot E) positions decreased, and the latter may reflect SOC transport out of the plot (see Section 3.1).

Prior to the I_2 event, the SOC concentration was once again significantly varied among slope positions ($P = 0.000$). For example, the

Table 1
Time pattern of sediment and runoff.

Sample no	1	2	3	4	5	6	7	8	9	10	11
Time (min)	7′34″	10′34″	13′34″	16′34″	19′34″	22′34″	25′34″	28′34″	31′34″	34′34″	36′34″
SYR-I$_1$ (g min^{-1})	0.09	0.67	1.59	1.37	1.43	0.23	1.45	1.47	1.55	1.41	
RR-I$_1$ (mm h^{-1})	4.34	26.20	43.00	47.00	44.00	51.00	50.00	48.00	52.50	52.50	13.50
SC-I$_1$ (g)	18.45	152.44	468.87	743.22	1029.31	1075.72	1365.92	1660.35	1969.47	2251.71	
RC-I$_1$ (L)	0.87	6.11	14.71	24.11	32.91	43.11	53.11	62.71	73.21	83.71	85.54
Time (min)	4′31″	7′31″	10′31″	13′31″	16′31″	19′31″	22′31″	25′31″	28′31″	31′31″	36′31″
SYR-I$_2$ (g min^{-1})	1.50	3.72	4.77	7.21	6.89	5.48	7.11	6.79	6.66	6.05	
RR-I$_2$ (mm h^{-1})	96.50	177.00	196.75	216.50	200.00	205.50	204.00	210.50	206.50	202.50	52.00
SC-I$_2$ (g)	299.92	1042.97	1997.21	3438.66	4816.66	5912.80	7335.50	8693.64	10025.98	11236.93	
RC-I$_2$ (g)	19.30	54.70	94.05	137.35	177.35	218.45	259.25	301.35	342.65	383.15	393.55

SYR-I$_1$, sediment yield rate for I$_1$ event; *RR*-I$_1$, runoff rate for I$_1$ event; *SC*-I$_1$, cumulative sediment yield for I$_1$ event; *RC*-I$_1$, cumulative runoff volume for I$_1$ event; *SYR*-I$_2$, sediment yield rate for I$_2$ event; *RR*-I$_2$, runoff rate for I$_2$ event; *SC*-I$_2$, cumulative sediment yield for I$_2$ event; *RC*-I$_2$, cumulative runoff volume for I$_2$ event

SOC concentration in subplot A was higher than in all other slopes, and that in subplot E was significantly lower ($P < 0.05$). Although it is not significant, a slight trend toward higher proportions of SOC at the bottom of the plot was observed in response to the I$_2$ rainfall. The SOC concentration in subplot A decreased, while that in the accumulation position of subplot E increased.

3.3. Vertical transport of SOC

Prior to the I$_1$ event, the SOC concentration showed distinct stratification with depth ($P < 0.01$), with the highest value in the surface layer (0–5 cm) regardless of the slope position ($P < 0.05$, except for subplot C; Fig. 5a). This indicates that SOC is concentrated in the soil surface, which is similar to the results of Jin et al. (2008). The SOC concentrations in the upper and middle slope positions (subplots A, B and C) showed similar vertical distributions, and they significantly decreased with depth for the 0–20 cm layers ($P < 0.01$, except for the first 0–10 cm of subplot C). In the 20–35 cm layer, SOC increased in subplots B and C ($P = 0.000$–0.007), while it decreased within subplot A. In subplot D the SOC concentrations in the 0–5 cm soil layer were significantly higher than those in the 5–10 cm layer; while SOC in the 10–20 cm layer was distinctively higher than in the 20–35 cm layer ($P = 0.000$). This indicates a possible burial process in the 10–20 cm layer. The SOC concentrations in subplot E decreased significantly with depth in each sampling layer ($P < 0.01$). The I$_1$ event significantly changed the vertical distribution of SOC within the 0–35 cm soil depth range (Fig. 5b). After the I$_1$ event, the 0–5 cm soil layer in subplot A exhibited the lowest SOC concentration, which then increased with depth until the 10–20 cm soil layer (0–5 versus 10–20 cm, $P = 0.021$). The SOC concentration then declined significantly in the 20–35 cm layer (10–20 versus 20–35 cm, $P = 0.036$). In the other subplots, the SOC concentrations in the 5–10 cm layer were always the lowest. Respective to increasing depths, the SOC concentrations then increased within the 10–20 cm layer. This trend was significant in subplots C (5–10 versus 10–20 cm, $P = 0.02$) and D (5–10 versus 20–35 cm, $P = 0.047$).

Table 2
Time pattern of sediment and runoff associated OC.

Sample no	1	2	3	4	5	6	7	8	9	10	11
Time (min)	7′34″	10′34″	13′34″	16′34″	19′34″	22′34″	25′34″	28′34″	31′34″	34′34″	36′34″
SCR-I$_1$ (g min^{-1})	0.01	0.07	0.34	0.18	0.01	0	0.07	0.01	0.14	0.24	
RCR-I$_1$ (mm h^{-1})	0.01	0.05	0.06	0.10	0.10	0.13	0.14	0.10	0.11	0.12	0.03
SCC-I$_1$ (g)	1.72	1.54	3.18	1.96	0.06	0	0.72	0.08	1.38	2.57	
RCC-I$_1$ (L)	30.45	26.53	20.40	30.53	34.17	39.61	41.69	30.74	30.04	34.93	31.06
Time (min)	4′31″	7′31″	10′31″	13′31″	16′31″	19′31″	22′31″	25′31″	28′31″	31′31″	36′31″
SCR-I$_2$ (g min^{-1})	1.71	4.22	2.50	3.28	2.78	0.93	0.69	1.05	1.54	0	
RCR-I$_2$ (mm h^{-1})	0.34	0.54	0.41	0.48	0.53	0.53	0.35	0.40	0.45	0.38	0.11
SCC-I$_2$ (g)	17.14	17.02	7.84	6.83	6.06	2.54	1.45	2.32	3.47	0	
RCC-I$_2$ (g)	53.33	45.69	31.05	33.03	39.83	38.74	25.38	28.63	32.99	27.78	32.47

SCR-I$_1$, sediment-associated OC yield rate for I$_1$ event; *RCR*-I$_1$, runoff-associated OC yield rate for I$_1$ event; *SCC*-I$_1$, sediment OC contents for I$_1$ event; *RCC*-I$_1$, runoff OC contents for I$_1$ event; *SCR*-I$_2$, sediment-associated OC yield rate for I$_2$ event; *RCR*-I$_2$, runoff-associated OC yield rate for I$_2$ event; *SCC*-I$_2$, sediment OC contents for I$_2$ event; *RCC*-I$_2$, runoff OC contents for I$_2$ event.

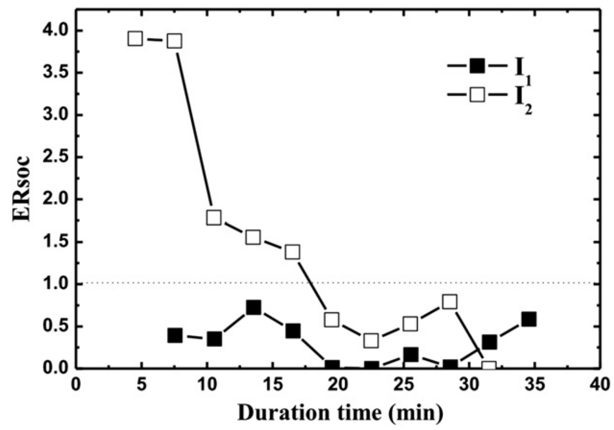

Fig. 3. Change in ER_{soc} with respect to time during the rainfall simulation experiments under different rainfall intensities (I_1: 0.58 mm min^{-1}; I_2: 1.64 mm min^{-1}).

Within the 10–20 and 20–35 cm depths, the SOC concentrations decreased similarly in all of the slope positions, except for subplot E.

Before the I_2 event, the SOC concentrations once more showed significant vertical stratification regardless of slope position ($P < 0.05$; Fig. 5c). SOC concentrations were the highest in the 0–5 and 5–10 cm layers, and then decreased markedly with respect to depth in the upper and middle slope positions of subplots A, B and C. In subplot D, the SOC concentrations in the 0–5 cm layer were also significantly higher than those in the 10–20 and 20–35 cm layers ($P = 0.000$). In subplot E, the highest SOC concentration was observed in the 20–35 cm layer (5–10 versus 20–35 cm, $P = 0.000$; 10–20 versus 20–35 cm, $P = 0.000$). Similar to the case of the I_1 event, this finding indicates SOC burial on the cultivated slope. During the I_2 event, soils displayed similar SOC vertical patterns (Fig. 5d). The SOC concentrations between 0 and 10 cm decreased with depth, only to then sharply increase towards their highest values within the 10–20 cm layer, a peak after which the SOC content decreases with depth, except for subplot E. In subplot E, SOC concentrations increased with depth for soils deeper than 10 cm. For subplots A, B, and C discrepancies among different depth layers were statistically significant (subplot A: 5–10 versus 10–20 cm, $P = 0.01$; 5–10 cm versus 20–35 cm, $P = 0.046$; subplot B: 0–5 cm versus 10–20 cm, $P = 0.017$; 0–5 cm versus 20–35 cm, $P = 0.033$; 5–10 cm versus 10–20 cm, $P = 0.011$; 5–10 cm versus 20–35 cm, $P = 0.021$; subplot C: 5–10 cm versus 10–20 cm, $P = 0.013$; 5–10 cm versus 20–35 cm, $P = 0.016$).

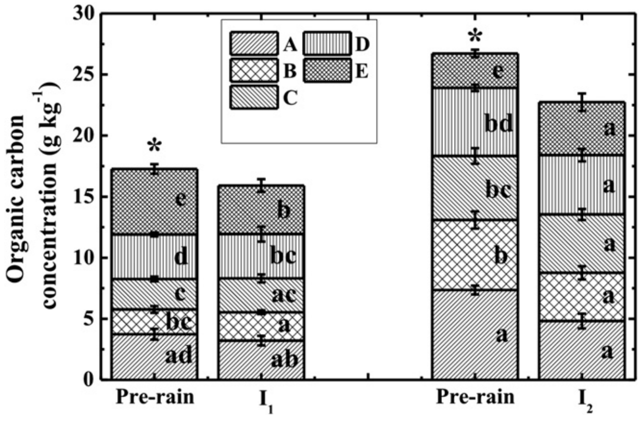

Fig. 4. Horizontal redistribution of soil organic carbon (SOC) in the 0–20 cm deep soil layer for pre- and post-rainfall of the I_1 and I_2 events (I_1: 0.58 mm min^{-1}; I_2: 1.64 mm min^{-1}). A to E represent subplots from the slope top to the toe located at 1 m intervals. The same letters (i.e., a to e) in a certain bar demonstrate no significant difference (LSD test, $\alpha = 0.05$). Error bars represent the standard error of the means ($n = 3$).

SOC concentrations decreased in the upper two layers (0–5 and 5–10 cm) after theI_1 event regardless of slope positions (Fig. 6a). This trend was statistically significant for the 0–5 and 5–10 cm layers of subplot A ($P = 0.002$) and the 5–10 cm layer for subplot C ($P = 0.031$). The SOC concentrations in the 10–20 and 20–35 cm layers became higher after the I_1 events, and the increase was significant for the 10–20 cm layer of subplot B ($P = 0.003$) (Fig. 6a). These findings confirm the vertical transport of SOC, a process which also occurred during the I_2 event (Fig. 6b). Except for subplot E, SOC concentrations decreased in the 0–5 and 5–10 cm layers, and increased in the 10–20 and 20–35 cm layers. The decrease was significant in the 5–10 cm layer of subplot A ($P = 0.008$), 0–5 and 5–10 cm layers of subplot B ($P = 0.006$ to 0.008), and the 0–5 cm layer of subplot C ($P = 0.001$). The increase was significant in the 10–20 cm layer of subplot B ($P = 0.042$), 10–20 and 20–35 cm layers of subplot C ($P = 0.005$ to 0.008), and the 10–20 cm of subplot D ($P = 0.043$). Although not significant, SOC concentrations increased regardless of soil depth in subplot E.

4. Discussion

The amounts of eroded SOC were found to be strongly influenced by rainfall intensity: more SOC was exported by the I_2 event than the I_1 event. This confirms that highly erosive rainstorms accelerate soil loss and the associated SOC loss. Erosion is an abrasive process. During the early period of the rainfall events, all the rain water was infiltrated and splash erosion dominated the soil loss process. Because of fast wetting and mechanical breakdown due to raindrop impacts (Shi et al., 2010), soil particles became more susceptible to splash erosion (Leguedois et al., 2005). During overland flow, inter-rill and rill erosion processes become dominant and runoff shear stress can slake the aggregate (Li et al., 2005). Erosion initially washes down small aggregates, then moving to larger ones. Large aggregates can also become fragmented by raindrops, then creating supply material for transport (Rodriguez et al., 2002; Schiettecatte et al., 2008). However, due to the lower SOC concentration in larger aggregates (Bronick and Lal, 2005), the SOC loss rate is shown to decrease (Table 2).

The SOC loss rate was not found to correlate with patterns of sediment and runoff loss (Tables 1 and 2). The loss rate of runoff-transported SOC was rather stable, and did not increase sharply with rainfall intensity. This does not apply to sediment-transported SOC, and higher rates occurred in the I_2 event than I_1 event (Table 2). Strong fluctuations in sediment-transported SOC during the I_2 event may reflect complex processes related to the decomposition of soil aggregates (Polyakov and Lal, 2008).

As noted earlier, sediment SOC losses during rainfall events can vary according to rainfall intensity, which agrees with the result of Truman et al. (2007). However, ER_{soc} was always lower than 1.0 during the I_1 event, and also after 18 min of the I_2 event. From this it can be seen that the more intense the erosive rainfall, the higher the enrichment ratio. This finding differs from some previous research results concerning sediment-transported SOC (Polyakov and Lal, 2004; Rumpel et al., 2006; Jin et al., 2009). According to Polyakov and Lal (2004), the higher ER_{soc} values obtained during the initial stage of the rainfall experiment are due to the flushing of loose organic particles and fine soil fractions. During the highly erosive I_2 event, large amounts of loose surface soils rich in SOC were transported first. Therefore, high ER_{soc} values were observed during the initial stage. Repeated sediment removal then led to mixing of the subsoil and topsoil, reducing the overall SOC concentration in the eroded sediment (Martínez-Mena et al., 2012) to levels even lower than in the undisturbed initial soil. Thus, ER_{soc} gradually decreased to lower than 1.0. In our research, the original soil SOC concentration was very low, according to the Second National Soil Survey, and had a rather high percentage of silt. As Jacinthe et al. (2004) have shown, the transport of SOC by erosion is related to the selective transport of finer soil particles. During this study,

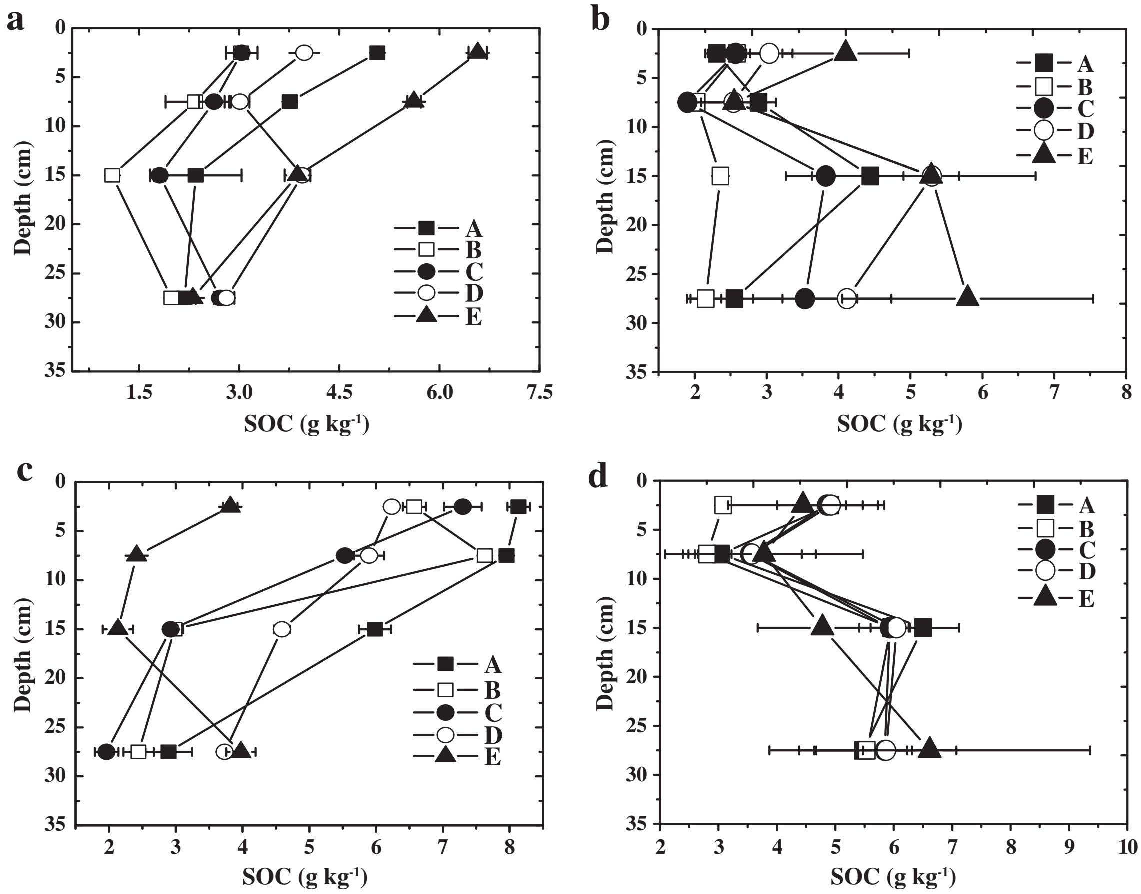

Fig. 5. Concentrations of soil organic carbon (SOC) before and after a rainfall simulation experiment for depths 0–5, 5–10, 10–20, and 20–35 cm. (a) Pre-rainfall, I_1 event. (b) Post-rainfall, I_1 event. (c) Pre-rainfall, I_2 event. (d) Post-rainfall, I_2 event. A to E represent subplots from the slope top to the toe located at 1 m intervals. Error bars represent the standard error of the means ($n = 3$).

however, a minimal amount of fine particles enriched in carbon (e.g., clay) were observed.

According to Strickland et al. (2005), the rainfall factors affecting detachment and transport thresholds for sediment and sediment-transported carbon also affect soil characteristics. Substantial carbon loss may only occur from storms above a certain threshold with short but intense rainfall events (Strickland et al., 2005; Truman et al., 2007). In the I_1 event, however, low ER_{soc} values were likely a result of the low concentrations of clay and SOC in conjunction with the lower intensity rainfall and eluviation of clay and organic matter into the soil during rainfall. At all events, a trend of horizontal transport from upper to lower slopes was observed regardless of rainfall intensity (Fig. 4), which agrees with the findings of Chaplot et al. (2005) and Van Oost et al. (2007).

Vertical SOC transport processes were found to affect the spatial distribution of SOC within the soil layers (Figs. 5 and 6). Before the

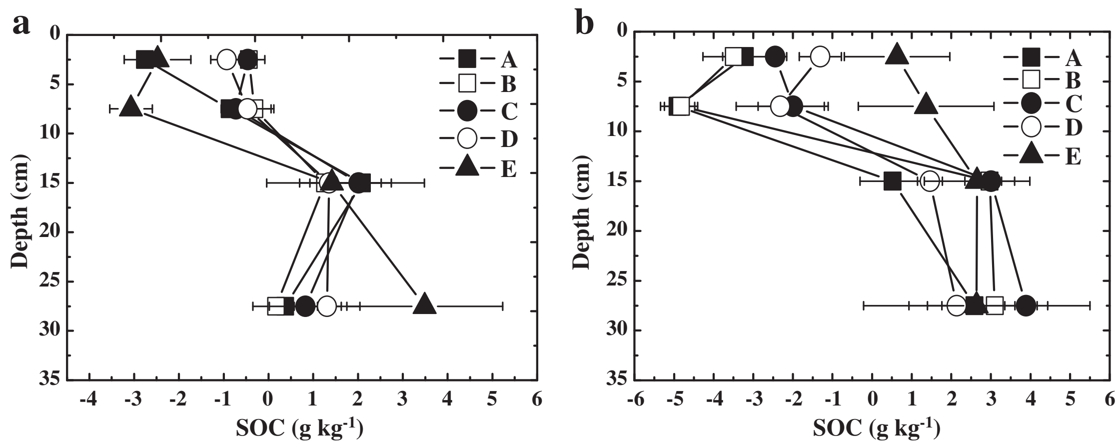

Fig. 6. Change in soil organic carbon (SOC) distribution due to rainfall simulation for depths of 0–5, 5–10, 10–20, and 20–35 cm. (a) I_1 event. (b) I_2 event. A to E represent subplots from the slope top to the toe located at 1 m intervals. The changes in SOC displayed represent the discrepancy between pre- and post-rainfall. Error bars represent the standard error of the means ($n = 3$).

rainfall simulations the SOC within the surface soil was enriched. After the simulations, a downward shift within SOC in the 0–5 and 5–10 cm soil layers and an upward shift within the 10–20 and 20–35 cm soil layers were observed. These SOC shifts are a direct result of infiltration at nearly all the slope positions (except subplot E during the I_2 event). Vertical transport within these plots was likely underestimated due to the assessment only being performed on the top 35 cm of soil. Deeper transport of clay and organic matter may have occurred. The incorporation of SOC deeper into the soil increases its potential for preservation, as evidenced by the somewhat high SOC concentrations observed in deep soil layers during long-term abandonment and erosion processes (e.g., the 20–35 cm soil layer in subplot E for the pre-I_2 event; Fig. 5c). Our data analysis has shown that three spatial transfer processes control the fate of eroded SOC. Although deeply buried SOC is relatively stable, carbon near the surface can easily be transported horizontally. After the exported SOC is transferred into the river network, it will comprise a more significant part of the larger scale carbon cycle. The lateral movement of carbon through the terrestrial system is a key uncertainty in our understanding of the carbon cycle (Stallard, 1998; Kuhn et al., 2009). The large scale carbon cycle can also be affected by complicated processes, including transport selectivity, as represented by different carbon enrichment ratios.

The results indicate that vertical leaching of SOC occurs more readily within shallow surface soils (0–10 cm) than in the deeper soils. From this, it could be inferred that higher rainfall intensities lead to a more significant vertical transport of SOC. Horizontal SOC transport can also become active under intense and erosive rainfall. Details about the contribution of vertical and horizontal processes on SOC transport should be examined within future work.

5. Conclusions

An expanded knowledge of vertical and lateral carbon flux is essential for a greater understanding of the carbon cycle. In the study area, eroded SOC was mobilized and redistributed throughout the slope surface and soil layers, or exported from the plot all together. Sediment-associated SOC played a major role in determining the total amount of SOC loss, with rainfall regimes significantly impacting the export process. Sediment ER_{soc} was also affected by rainfall intensity. Sediment-enriched SOC, however, was not obvious in the study area due to the low SOC concentration of the original soils, the low rainfall intensity, and the eluviation of clay and organic matter into the soil. Although not always significant, horizontal on-site redistribution of SOC occurred regardless of rainfall intensity. SOC was also transported from the upper to deeper soil layers via infiltration, resulting in vertical variabilities of SOC regardless of slope positions. Due to these transport processes, the part of eroded SOC was either deposited near the soil surface or deeper into the soil layers.

Acknowledgments

The study was funded by the National Natural Science Foundation of China (40971179, 41271294), the Program for New Century Excellent Talents in University (NCET-09-330), and the Natural Science Foundation of Hunan Province of China (11JJ3041).

References

Bronick, C., Lal, R., 2005. Soil structure and management: a review. Geoderma 124, 3–22.
Chaplot, V.A.M., Rumpel, C., Valentin, C., 2005. Water erosion impact on soil and carbon redistributions within uplands of MekongRiver. Global Biogeochemical Cycles 19, GB4004. http://dx.doi.org/10.1029/2005GB002493.
Engel, F.L., Bertol, I., Ritter, S.R., Paz González, A., Paz-Ferreiro, J., Vidal Vázquez, E., 2009. Soil erosion under simulated rainfall in relation to phenological stages of soybeans and tillage methods in Lages, SC, Brazil. Soil and Tillage Research 103, 216–221.
Foster, G.R., Wischmeier, W.H., 1974. Evaluating irregular slopes for soil loss prediction. Transactions of the American Society of Agricultural Engineers 17, 305–309.
Gee, G.W., Bauder, J.W., 1986. Particle size analysis, In: Klute, A. (Ed.), Methods of Soil Analysis, 2nd ed. Am. Soc. Agron, Madison, pp. 383–411.
Heckrath, G.D., Quine, J., Van Oost, T.A., Govers, K., Zhang, G., 2005. Tillage erosion and its effect on soil properties and crop yield in Denmark. Journal of Environmental Quality 34, 312–324.
Jacinthe, P.A., Lal, R., Owens, L., Hothem, D., 2004. Transport of labile carbon in runoff as affected by land use and rainfall characteristics. Soil and Tillage Research 77, 111–123.
Jin, K., Cornelis, W.M., Schiette, W., Lu, J., Buysse, T., Baert, G., Wu, H., Yao, Y., Cai, D., Jin, J., 2008. Redistribution and loss of soil organic carbon by overland flow under various soil management practices on the Chinese Loess Plateau. Soil Use and Management 24, 181–191.
Jin, K., Cornelis, W.M., Gabriels, D., Baert, M., Wu, H.J., Schiettecatte, W., Cai, D.X., De Neve, S., Jin, J.Y., Hartmann, R., Hofman, G., 2009. Residue cover and rainfall intensity effects on runoff soil organic carbon losses. Catena 78, 81–86.
Kara, D., Özsavasçi, C., Alkan, M., 1997. Investigation of suitable digestion methods for the determination of total phosphorus in soils. Talanta 44, 2027–2032.
Kjeldahl, J., 1883. Neue methode zurestimmung des stickstoffs in organischen kÖrpen. Zeitschrift für Analytische Chemie 22, 366–382.
Kuhn, N.J., Hoffmann, T., Schwanghart, W., Dotterweich, M., 2009. Agricultural soil erosion and global carbon cycle: controversy over? Earth Surface Processes and Landforms 34, 1033–1038.
Lal, R., 2003. Soil erosion and the global carbon budget. Environment International 29, 437–450.
Lal, R., Pimentel, D., 2008. Soil erosion: a carbon sink or source? Science 319, 1040–1042.
Lal, R., Henderlong, P., Flowers, M., 1998. Forages and row cropping effects on soil organic carbon and nitrogen contents. In: Lal, R., Kimble, J.M., Follett, R.F., Stewart, B.A. (Eds.), Management of Carbon Sequestration in Soil. CRC Pres Inc., Columbus, pp. 365–379.
Leguedois, S., Planchon, O., Legout, C., Bissonnais, Y.L., 2005. Splash projection distance for aggregated soils: theory and experiment. Soil Science Society of America Journal 69, 30–37.
Li, Z.X., Cai, C.F., Shi, Z.H., Wang, T.W., 2005. Aggregate stability and its relationship with some chemical properties of red soils in subtropical China. Pedosphere 15, 129–136.
Martínez-Mena, M., López, J., Almagro, M., Albaladejo, J., Castillo, V., Ortiz, R., Fayos, C.B., 2012. Organic carbon enrichment in sediments: effects of rainfall characteristics under different land uses in a Mediterranean area. Catena 94, 36–42.
McCarty, G.W., Ritchie, J.C., 2002. Impact of soil movement on carbon sequestration in agricultural ecosystems. Environmental Pollution 116, 423–430.
Pan, C., Shangguan, Z., 2006. Runoff hydraulic characteristics and sediment generation in sloped grassplots under simulated rainfall conditions. Journal of Hydrology 331, 178–185.
Papiernik, S.K., Lindstrom, M.J., Schumacher, J.A., Farenhorst, A., Stephens, K.D., Schumacher, T.E., Lobb, D.A., 2005. Variation in soil properties and crop yield across an eroded prairie landscape. Journal of Soil and Water Conservation 60, 388–395.
Papiernik, S.K., Lindstrom, M.J., Schumacher, T.E., Schumacher, J.A., Malo, D.D., Lobb, D.A., 2007. Characterization of soil profiles in a landscape affected by long-term tillage. Soil and Tillage Research 93, 335–345.
Polyakov, V.O., Lal, R., 2004. Soil erosion and carbon dynamics under simulated rainfall. Soil Science 169, 590–599.
Polyakov, V.O., Lal, R., 2008. Soil organic matter and CO_2 emission as affected by water erosion on field runoff plots. Geoderma 143, 216–222.
Rimal, B.K., Lal, R., 2009. Soil and carbon losses from five different land management areas under simulated rainfall. Soil and Tillage Research 106, 62–70.
Rodriguez, A.R., Guerra, J.A., Gorrin, S.P., Arbelo, C.D., Mora, J.L., 2002. Aggregates stability and water erosion in Andosols of the Canary Islands. Land Degradation & Development 13, 515–523.
Rumpel, C., Chaplot, V., Planchon, O., Bernadou, J., Valentin, C., Mariotti, A., 2006. Preferential erosion of black carbon on steep slopes with slash and burn agriculture. Catena 65, 30–40.
Rumpel, C., Ba, A., Darboux, F., Chaplot, V., Planchon, O., 2009. Erosion budget and process selectivity of black carbon at meter scale. Geoderma 154, 131–137.
Schiettecatte, W., Gabri ls, D., Cornelis, W., Hofman, G., 2008. Enrichment of organic carbon in sediment transport by interrill and rill erosion processes. Soil Science Society of America Journal 72, 50–55.
Seybold, C., Hubbs, M., Tyler, D., 2002. On-farm tests indicate effects of long-term tillage systems on soil quality. Journal of Sustainable Agriculture 19, 61–73.
Shi, Z.H., Yan, F.L., Li, L., Li, Z.X., Cai, C.F., 2010. Interrill erosion from disturbed and undisturbed samples in relation to topsoil aggregate stability in red soils from subtropical China. Catena 81, 240–248.
Stallard, R.F., 1998. Terrestrial sedimentation and the carbon cycle: coupling weathering and erosion to carbon burial. Global Biogeochemical Cycles 12, 231–257.
Strickland, T.C., Truman, C.C., Frauenfeld, B., 2005. Variable rainfall intensity effects on carbon characteristics of eroded sediments from two coastal plain ultisols in Georgia. Journal of Soil and Water Conservation 60, 142–148.
Tang, K.L., 2004. China Soil and Water Conservation. Science Press, Beijing, China (In Chinese).
Truman, C.C., Strickland, T.C., Potter, T.L., Franklin, D.H., Bosch, D.D., Bednarz, C.W., 2007. Variable rainfall intensity and tillage effects on runoff, sediment, and carbon losses from a loamy sand under simulated rainfall. Journal of Environmental Quality 36, 1495–1502.

Van Oost, K., Quine, T.A., Govers, G., De Gryze, S., Six, J., Harden, J.W., Ritchie, J.C., McCarty, G.W., Heckrath, G., Kosmas, C., 2007. The impact of agricultural soil erosion on the global carbon cycle. Science 318, 626–629.

Walkley, A., Black, I.A., 1934. An examination of the Degtjareff method for determining soil organic matter, and a proposed modification of the chromic acid titration method. Soil Science 37, 29–38.

Yang, F., Tang, X.N., Xiao, Z.H., Yu, T.W., 1989. Hunan Soils. Agriculture Press, Beijing (in Chinese).

Zhao, Q.G., 2002. The Red Soil Material Cycling and its Regulation. Science Press, Beijing (in Chinese).